CrossMark

ORIGINAL ARTICLE

NMR-Based Metabolomics Separates the Distinct Stages of Disease in a Chronic Relapsing Model of Multiple Sclerosis

Alex M. Dickens[1,2,3] · James R. Larkin[1] · Benjamin G. Davis[3] · Julian L. Griffin[4] ·
Timothy D. W. Claridge[3] · Nicola R. Sibson[1] · Daniel C. Anthony[2]

Abstract Relapsing experimental allergic encephalomyelitis (Cr-EAE) is commonly used to explore the pathogenesis and efficacy of new therapies for MS, but it is unclear whether the metabolome of Cr-EAE is comparable to human multiple sclerosis (MS). For MS, the diagnosis and staging can be achieved by metabolomics on blood using a combination of magnetic resonance spectroscopy and partial least squares discriminant analysis (PLS-DA). Here, we sought to discover whether this approach could be used to differentiate between sequential disease states in Cr-EAE and whether the same metabolites would be discriminatory. Urine and plasma samples were obtained at different time-points from a clinically relevant model of MS. Using PLS-DA modelling for the urine samples furnished some predictive models, but could not discriminate between all disease states. However, PLS-DA modelling of the plasma samples was able to distinguish between animals with clinically silent disease (day 10, 28) and animals with active disease (day 14, 38). We were also able to distinguish Cr-EAE mice from naive mice at all-time points and control mice, treated with complete Freund's adjuvant alone, at day 14 and 38. Key metabolites that underpin these models included fatty acids, glucose and taurine. Two of these metabolites, fatty acids and glucose, were also key metabolites in separating relapsing-remitting MS from secondary-progressive MS in the human study. These results demonstrate the sensitivity of this metabolomics approach for distinguishing between different disease states. Furthermore, some, but not all, of the changes in metabolites were conserved in humans and the mouse model, which could be useful for future drug development.

Keywords Metabolomics · Experimental allergic encephalomyelitis · Multiple sclerosis · Diagnostics · Mouse

Alex M. Dickens and James R. Larkin contributed equally to this work.

Electronic supplementary material The online version of this article (doi:10.1007/s11481-015-9622-0) contains supplementary material, which is available to authorized users.

✉ Nicola R. Sibson
   nicola.sibson@oncology.ox.ac.uk

[1] Cancer Research UK and Medical Research Council Oxford Institute for Radiation Oncology, Department of Oncology, Radiobiology Research Institute, Churchill Hospital, University of Oxford, Oxford OX3 7LJ, UK

[2] Department of Pharmacology, University of Oxford, Oxford OX1 3QT, UK

[3] Department of Chemistry, University of Oxford, Oxford OX1 3TA, UK

[4] Department of Biochemistry, University of Cambridge, Oxford CB2 1GA, UK

Introduction

Multiple sclerosis (MS) is the commonest cause of progressive disability in the western world (Noseworthy et al. 2000), but our understanding of the underlying mechanisms responsible for the clinical course, including the transition from relapsing to progressive disease remain elusive (Bielekova and Martin 2004). Identifying biomarkers within biofluids is considered a useful way to generate surrogate makers of disease activity and to explore possible pathogenic mechanisms. Urine and blood from patients with neurological disease, including MS, have been assayed for disease-specific markers, such as myelin basic protein-derived material indicating demyelination (Whitaker et al. 1994; Whitaker et al. 1995) or neopterin as a marker of CNS inflammation (Ott et al. 1993; Giovannoni et al. 1997). However, these studies focussed on

the detection of either a single or a small number of specific metabolites and although differences have been identified at a group level, predictive value at an individual level has been low (Kuhle et al. 2011).

The use of high field ^{1}H-NMR on biofluid samples is becoming more prevalent within the literature to asses drug toxicity and to profile of disease activity (Hassan-Smith et al. 2012; Heather et al. 2012; Barallobre-Barreiro et al. 2013; Meyer et al. 2013). This metabolomic approach of biofluid profiling and statistical pattern recognition requires no a priori knowledge, but rather identifies metabolites solely according to their correlated variation between treatment groups (Lindon et al. 2001). Techniques such as principal components analysis (PCA) can identify distinct patterns of metabolites whose variation as a whole is characteristic of the disease, rather than requiring identification of a unique biomarker (Lindon et al. 2001). Partial least squares-discriminant analysis (PLS-DA) modelling is a class based modelling system that generates separations in the data based on user-defined classes (Lindon et al. 2001). Therefore, PLS-DA modelling removes the influences of non-disease specific changes. These factors could be a range of co-variables such as gender specific metabolite changes and drug treatment effects (Salek et al. 2010).

We have previously shown that it is possible to use such approaches to distinguish between groups of animals injected intracerebrally with replication-deficient recombinant adenoviruses expressing either TNF-α or IL-1β simply through analysis of their urine (Griffin et al. 2004). These two adenoviruses induce markedly different lesions in the brain with TNF-α inducing a predominantly macrophage-mediated pathology and IL-1β a neutrophil-rich lesion. Using ^{1}H-NMR spectroscopy of the urine samples, coupled with PLS-DA, clear separation of the groups was evident. This finding suggests that the ^{1}H-NMR/PLS-DA approach may be highly sensitive not just to the presence of pathology within the brain, but to differences and/or changes in pathological processes. Furthermore, we have recently demonstrated that it is possible to separate relapsing-remitting (RR) MS from secondary-progressive (SP) MS using this technique on serum obtained from MS patients (Dickens et al. 2014). The conversion from the RR to SP stage is the key determinant of prognosis and its prevention or delay is a major therapeutic target. Since the optimal therapeutic strategies are markedly different between these two disease states the ability to definitively categorise patients is critical for treatment. The separation of RR from SP will have important clinical utility. However, our case-controlled study in humans did not enable interrogation of the relapsing-remitting cycle with the level of granularity that can be afforded by the use of a Cr-EAE model and serial sampling.

Experimental allergic encephalomyelitis (EAE), an auto-immune inflammatory disease of the central nervous system (CNS), is a model for the human disease multiple sclerosis

(MS) (Lassmann 1983; Alvord 1984). The initial models displayed acute monophasic disease, but chronic relapsing forms of murine EAE (CrEAE) have been produced by adapting the immunization schedule and by selection of the mouse strain used (Brown and McFarlin 1981; Mokhtarian et al. 1984; Zamvil et al. 1985). The Biozzi mice were selectively bred by Guido Biozzi in 1972 to produce mice with a high antibody response to sheep red blood cells; these mice are susceptible to EAE and develop a chronic relapsing pattern of disease characterized by lymphocyte infiltration of the CNS, with demyelination being particularly evident in relapse (Amor et al. 2005). As in human MS, the trigger for relapse is poorly understood, but it is clear that different pathogenic mechanisms appear to underlie the first and second phases of disease. For example, radiological signs are ameliorated by anti-IL-17A in the first phase of disease, but not so markedly in the relapse (Mardiguian et al. 2013).

The aims of the current study, therefore, were to determine whether the combined ^{1}H-NMR/PLS-DA analysis of blood and/or urine samples in the Cr-EAE model could (i) identify changes in the metabolite profile prior to the appearance of clinical signs of disease, and (ii) differentiate between different (relapse/remission) phases of disease.

Materials and Methods

Animal Model

Urine and plasma samples were obtained from a mouse model of chronic relapsing experimental autoimmune encephalomyelitis (Cr-EAE), a more clinically-relevant model for MS than the commonly used monophasic disease models (Jackson et al. 2009). Adult Biozzi ABH mice were fed on a diet of jelly and high protein mash in the cage to ensure adequate food and hydration at the point of paralysis, when the animals can no longer reach the overhead food and water supply. Animals were acclimatised to this diet for a period of one week prior to Cr-EAE induction. Cr-EAE was induced as described by Baker and co-workers (Baker et al. 1990). Briefly, each animal was injected subcutaneously on day 0 and day 7 with mouse spinal cord homogenate in incomplete Freund's adjuvant supplemented with non-viable desiccated, *M. tuberculosis* (4 mg/ml) and *M. butyricum* (1 mg/ml) to produce a complete Freund's adjuvant (CFA). A group of control animals (CFA) was injected with our CFA, but omitting the spinal cord homogenate. Animals were weighed daily and assessed for clinical signs using the following scoring system: 0, healthy animal; 1, tail paralysis; 2, weakness in hind limbs, 3; total hind limb paralysis, 4; full limb paralysis as previously described in (Serres et al. 2011).

Biofluid Samples

Blood samples (0.5 mL) were taken at days 10, 14, 28 and 38 after Cr-EAE induction ($n=10$, 8, 9, 8 and 5 respectively for the Cr-EAE cohort and $n=8$, 9, 8, 9 and 8 for the CFA control cohort). Urine samples were collected from the animals at the same time points ($n=8$, 7, 0, 7 and 6 for the Cr-EAE cohort and $n=6$, 10, 0, 8 and 10 for the CFA control cohort respectively). Blood and urine samples were also collected from naïve animals (blood $n=18$, urine $n=15$). Blood was collected by cardiac puncture using a heparin-coated syringe and placed immediately into a blood tube containing dipotassium ethylenediaminetetraacetic acid (EDTA, Teklab, UK) on ice. Blood samples were separated by centrifugation (3000 g, 5 min, 4 °C), and the layer of plasma was removed and stored at −80 °C. Urine samples were either collected directly from the bladder after sacrificing the animal with CO_2 or by placing a 96-well plate underneath the animal during sacrifice.

NMR Spectroscopy

Urine or blood plasma samples were defrosted overnight in a cold room prior to the NMR experiments and then blood samples were further centrifuged (100,000 g, 30 min, 4 °C). The urine and plasma samples (100 μL) were placed in a 5 mm NMR tube and diluted to a final volume of 600 μL with phosphate buffer (0.2 M Na_2HPO_4/0.04 NaH_2PO_4, pH 7.4, 0.1 % sodium azide, 0.8 % sodium chloride) in D_2O containing 1 mM TSP (3-trimethylsilyl-1-[2,2,3,3,-$^2H_4$] propionate) as an internal standard. ^1H-NMR spectra were acquired from each sample using a 16.4 T NMR (700 MHz ^1H) system (Bruker Avance III equipped with a ^1H TCI cryoprobe). For all samples a 1D NOESY pre-saturation sequence, with solvent pre-saturation during the relaxation delay (2 s) and mixing time (10 ms), was used. Two dimensional ^1H-NMR spectra were acquired from a sample within each group to assist with metabolite identification. The 2D Correlation Spectroscopy (COSY) spectra were acquired on the same spectrometer as the 1D NMR spectra. The COSY spectra were acquired with 1.5 s solvent presaturation, a spectral width of 10 ppm (7002 Hz), and 16 or 32 transients per t_1 increment for 256 increments. All NMR experiments were acquired at 293 K.

Data Analysis

The 1D ^1H spectra were imported into MATLAB (Mathworks) automatically phased using a method optimised for signal-dense spectra (Bao et al. 2013). Spectra were inspected for gross distortions or phasing errors and discarded as necessary at this point. Spectra were baseline corrected by fitting a third order polynomial to regions without peaks before alignment and scaling to the TSP peak at 0.0 ppm. Coarsely aligned spectra were subjected to non-linear warping

to correct minor shift changes arising due to pH or ionic strength changes (Skov et al. 2006). Processed spectra were sub-divided into 0.02 pm regions (δ=midpoint of integral region) and integrated using an in-house MATLAB script. Serum and plasma spectra were thus reduced to 435 independent variables between 0.20–4.30 and 5.00–9.60 ppm, whilst the urine spectra were reduced to 385 independent variables between 0.20–4.30 and 6.00–9.60 ppm. In all spectra, the region between 4.30 and 5.00 ppm was omitted due to spectrum distortion arising from the water suppression at 4.7 ppm. In the urine spectra the region between 5.00 and 6.00 ppm was also excluded to avoid the broad resonance arising from urea. These sections represent highly variable regions of the spectrum. All data were scaled using the Pareto variance to suppress noise in the data. Subsequently, statistical pattern recognition was applied to the spectra to differentiate between samples obtained from different disease states in the Cr-EAE model.

Statistical Methods

For each group comparison, a partial least squares discriminant analysis (PLS-DA) model was derived which best explained the differences between the groups being studied (SIMCA P+ 13.0, Umetrics, Sweden). To determine how predictive the models were likely to be, the q^2 value was used. q^2 is a value derived from a step-wise cross-validation of the model whereby a fraction of the samples are removed, the model re-built and the new model used to predict the class of the removed samples. Specifically, q^2 represents the predicted residual sum of squares (PRESS) divided by the initial sum of squares and subtracted from 1. A value of $q^2>0$ means that the model is predictive and it is generally held that a value of >0.4 is the threshold for significance for biological modelling (Waterman et al. 2010).

In addition to using the q^2 values, model validation was carried out within SIMCA using a pseudo-Monte Carlo method. To achieve this, 100 models were built with the samples assigned to random groups. The goodness of fit of each of these randomly permuted models was compared to the fit for the genuine model. Only models where the genuine q^2 value was higher than 95 % or more of the randomly generated q^2 values were considered predictive.

Metabolite Identification

In order to identify the metabolites the loadings were examined by use of an s-plot, and the peaks were identified using a combination of COSY spectroscopy (Supplemental Information 1), literature values and reference to the human metabolome database (see Supplementary Information 2) for full NMR assignments) (Fan 1996; Wishart et al. 2007; Wishart et al. 2009). Further confirmation of the metabolites was achieved by examining the *J*-coupling (spin-spin

interactions between neighbouring hydrogens) of the resonances within the spectra.

In order to confirm the identity of the singlet peaks which give no correlations within the 2D COSY spectra the predicted metabolite was added ('spiked') into the NMR tube as an authentic reference sample.

Results

Cr-EAE: Animal Model

All Cr-EAE animals followed the typical disease course reported previously by Baker et al. 1990; the animals exhibited significant weight loss and increased clinical score, which peaked at day 17, and was followed by full remission such that clinical score had returned to baseline values in all animals by day 26 (Fig. 1). Subsequently, the animals entered a relapse phase, around day 32, with a second significant increase in clinical score and loss of weight. During peak disease Cr-EAE animals were hand-fed to reduce dehydration and weight loss. Injection of CFA alone (CFA group) did

(A)

(B)
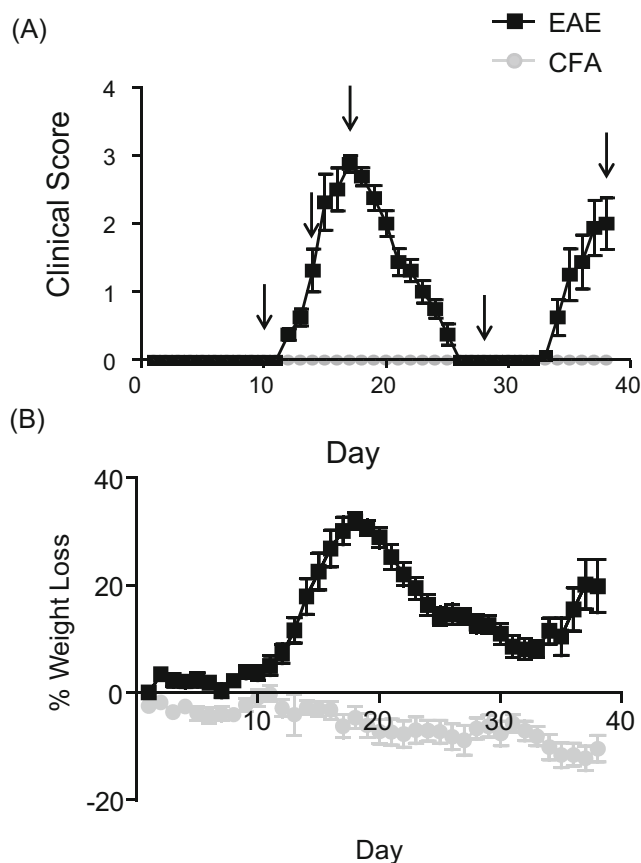
Fig. 1 **a** A graph showing the clinical scores of the mice with Cr-EAE and CFA alone. Arrows indicate when the samples were taken from each animal. **b** A graph showing the percentage weight loss of the both the Cr-EAE and CFA animals

Fig. 2 EAE urine model results **a** ^{1}H NMR NOESY-presat spectrum of a urine sample from a Day 38 animal. **b** PLS-DA plot of animal urine samples comparing EAE animals at Day 38 (*black squares*) and EAE animals at Day 28 (*grey squares*). **c** PLS-DA plot of animal urine samples comparing EAE animals at Day 38 (*black squares*) and naïve animals (*grey triangles*). **d** PLS-DA plot of animal urine samples comparing EAE animals at Day 38 (*black squares*) and CFA animals at Day 38 (*grey circles*) **e** Table showing the q^2 values of all the animal models along with key metabolites identified. Values on the white background shows the EAE v EAE comparison, values on a light grey background shows the EAE v CFA comparisons and the values on the dark grey background shows the CFA v CFA comparisons. **f** Table to show the q^2 values of EAE and CFA animals at different time points compared to a naïve group of animals along with key metabolites identified. n.p. = not predictive (i.e., q^2 value<0)

not cause any overt clinical signs or significant weight loss (Fig. 1). However, the injection of CFA does induce an immunological response in the animals (Billiau and Matthys 2001) and, therefore, an additional naïve control group was used to tease out metabolite changes due to the CFA injection alone.

Cr-EAE: Urine Analysis

Spectra obtained by ^{1}H-NMR spectroscopy were of sufficient resolution to allow identification of over 30 metabolites (Fig. 2a). PLS-DA analysis of the urine spectra from the naive animals at different time-points returned a model with a low q^2 (0.10), indicating that it was not significantly predictive. Consequently, all naïve data were combined thereafter and analysis performed using a single control (naïve) group.

Visually, there appeared to be separation of the different disease groups, as illustrated in Fig. 2 b, c and d. However, although many of the urine models returned a positive q^2 value indicating differences both within the Cr-EAE animals at different time-points and between the Cr-EAE and control (CFA or naïve) animals, only 12 models reached statistical significance against the defined criteria of $q^2 \geq 0.4$ (Fig. 2; Tables E and F). At day 10 it was possible to separate both the Cr-EAE and the CFA animals from the naïve animals ($q^2 = 0.55$ and 0.53, respectively; Fig. 2; Tables E and F) although, whilst strongly positive, the separation between Cr-EAE and CFA animals at this time-point did not quite reach the defined significance ($q^2 = 0.38$). However, a significant separation was found between the Cr-EAE and CFA animals at day 14 with a q^2 value of 0.46 (Fig. 2; Table E). Cr-EAE animals at day 38 showed a positive separation from all other Cr-EAE time-points and also from the CFA and naïve controls (Fig. 2, Tables E and F).

CFA animals at day 10 showed a positive separation from both days 14 and 38 ($q^2 = 0.47$ and 0.5, respectively; Fig. 2; Table E), and at day 28 the CFA animals showed a separation from the naïve cohort ($q^2 = 0.5$; Fig. 2; Table F).

E
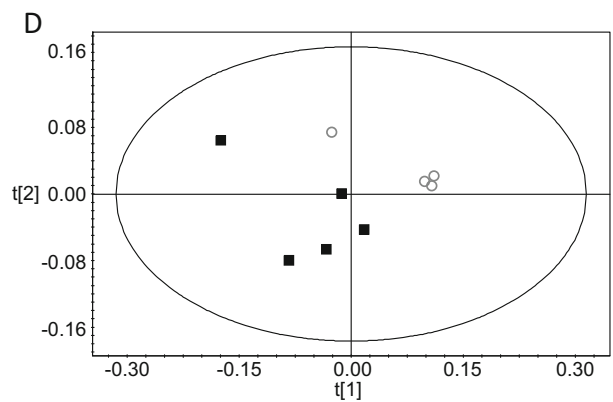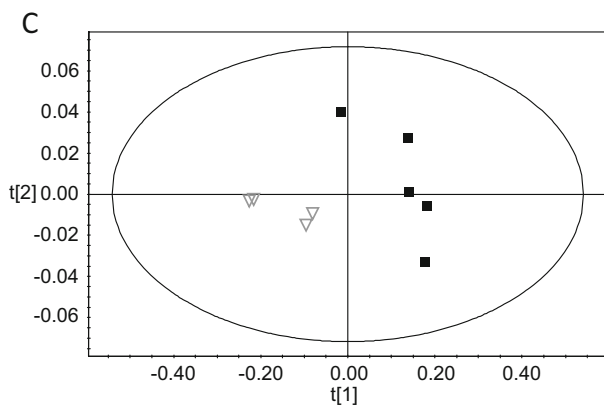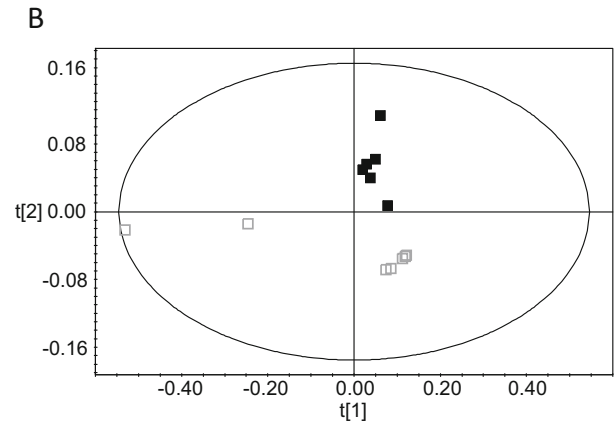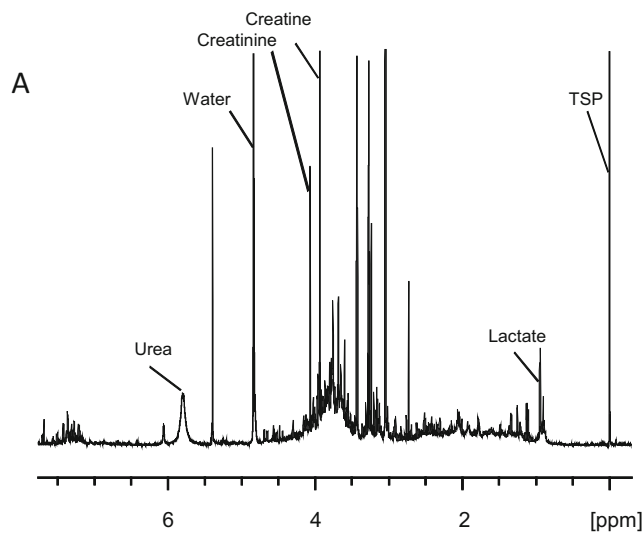
	Day 10	Day 14	Day 28	Day 38
q²	n.p.	0.21	n.p.	0.79
Day 10 ↑			TMAO; citrate; creatine	
↓			Trimethylamine; ureidopropionic acid; taurine	
q²	0.47	0.46	n.p.	0.52
Day 14 ↑		Creatine; creatinine; glucose	TMAO; citrate	
↓		Citrate		
q²	n.p.	n.p.	n.p.	0.76
Day 28 ↑				
↓			TMAO; citrate	
q²	0.50	n.p.	n.p.	0.52
Day 38 ↑			TMAO; citrate; phosphocholine; glucose	
↓			Creatine	

F

		EAE vs Naïve	CFA vs Naïve
	q²	0.55	0.53
Day 10	↑	Creatinine; trimethylamine; TMAO; ureidopropionic acid	
	↓	Citrate	
Day 14	q²	n.p.	n.p.
	q²	0.19	0.50
Day 28	↑		
	↓		
	q²	0.77	0.66
Day 38	↑	TMAO; glucose; creatine	
	↓		Citrate

EAE vs EAE | EAE vs CFA | CFA vs CFA

The loadings from the statistically significant models generated for the disease time course identified several key metabolites that were responsible for the separations between groups (see Supplemental Information 2 for full literature assignments). Here δ_{x-y} is defined as the chemical shift of the centre of the integral range used as a variable. In particular,

citrate (δ_{x-y} 2.50, 2.65), creatine (δ_{x-y} 3.03), taurine (δ_{x-y} 3.25, 3.40), an unassigned set of resonances (δ_{x-y} 3.13, two singlets in close proximity to each other), trimethylamine-N-oxide (TMAO; δ_{x-y} 3.26), trimethylamine (TMA; δ_{x-y} 2.89) and ureidopropionic acid (δ_{x-y} 2.37) all varied significantly over the disease time course. The identity of these last three metabolites was confirmed by spiking experiments (Fig. 3). With the exception of ureidopropionic acid, the same metabolites were also identified when comparing Cr-EAE animals with the two control groups (CFA and naïve). In addition, phosphocholine (δ_{x-y} 3.23), also confirmed by spiking (Fig. 3d), was an important contributor to the model separating Cr-EAE and CFA animals at day 38. For detailed metabolite changes see Fig. 2e.

Cr-EAE: Plasma Analysis

As for the urine, PLS-DA analysis of the plasma spectra from the naive animals at different time-points returned a model with a low q^2 (0.176), indicating that it was not significantly predictive. Consequently, all naïve data were combined thereafter and analysis performed using a single control (naïve) group.

Although the spectra from all groups looked superficially similar upon initial overlay, the multi-variant statistical analysis of the data sets showed predictive separations between the Cr-EAE at all-time points when plasma was collected. It was also possible to generate predictive models that separated the Cr-EAE and CFA control groups at days 14 and 38 when the animals were showing overt clinical signs. It was not possible to separate out the Cr-EAE animals from the CFA controls at day 10 and day 28 when the disease is clinically silent. However, it was possible to generate predictive models

between the EAE animals and the naïve controls (Fig. 4e). It was also possible to generate predictive models based on the spectra from the plasma of the CFA animals across the time course (Fig. 4e).

On examination of the loadings within the PLS-DA models for the Cr-EAE time course several key metabolites were identified as generating the positive separations. The models showed variations in broad resonances likely to be fatty acids (δ_{x-y} 0.88, 1.58, 2.03), taurine (δ_{x-y} 3.25), lactate (δ_{x-y} 1.32), TMAO (δ_{x-y} 3.26), choline (δ_{x-y} 3.22), phosphocholine (δ_{x-y} 3.23) and glucose (δ_{x-y} 3.26, 5.25). For detailed changes see Fig. 4e.

Key metabolites from the original models separating Cr-EAE animals from the control groups (CFA or naïve) were also identified. The metabolites that showed greatest variation in these models were: fatty acids (δ_{x-y} 0.88, 1.58, 2.03), lactate (δ_{x-y} 1.32, 4.11), glucose (δ_{x-y} 3.25) and phosphocholine (δ_{x-y} 3.23). When the data from CFA

Fig. 4 EAE plasma model results **a** ^{1}H NMR NOESY-presat spectrum of an EAE animal plasma sample at Day 38. **b** PLS-DA plot of animal plasma samples comparing EAE animals at Day 38 (*black squares*) and EAE animals at Day 28 (*grey squares*). **c** PLS-DA plot of animal plasma samples comparing EAE animals at Day 38 (*black squares*) and naïve animals (*grey triangles*). **d** PLS-DA plot of animal plasma samples comparing EAE animals at Day 38 (*black squares*) and CFA animals at Day 38 (*grey circles*) **e** Table showing the q^2 values of all the animal models along with key metabolites identified. Values on the white background shows the EAE v EAE comparison, values on a light grey background shows the EAE v CFA comparisons and the values on the dark grey background shows the CFA v CFA comparisons. **f** Table showing the q^2 values of EAE animals at different time points compared to a naïve group of animals along with key metabolites identified

Fig. 3 Urine NMR spiking experiments. ^{1}H NMR spectrum of potential metabolites in order to confirm the identity of metabolites with a singlet resonance. (**a**, *orange*) Baseline ^{1}H NMR NOESY of animal urine. (**b**, *purple*) Addition of ureidopropionic acid. (**c**, *red*) Addition of TMAO. (**d**, *Green*) Addition of phosphocholine. (**e**, *blue*) Addition of TMA

Panel E — EAE vs EAE / EAE vs CFA / CFA vs CFA
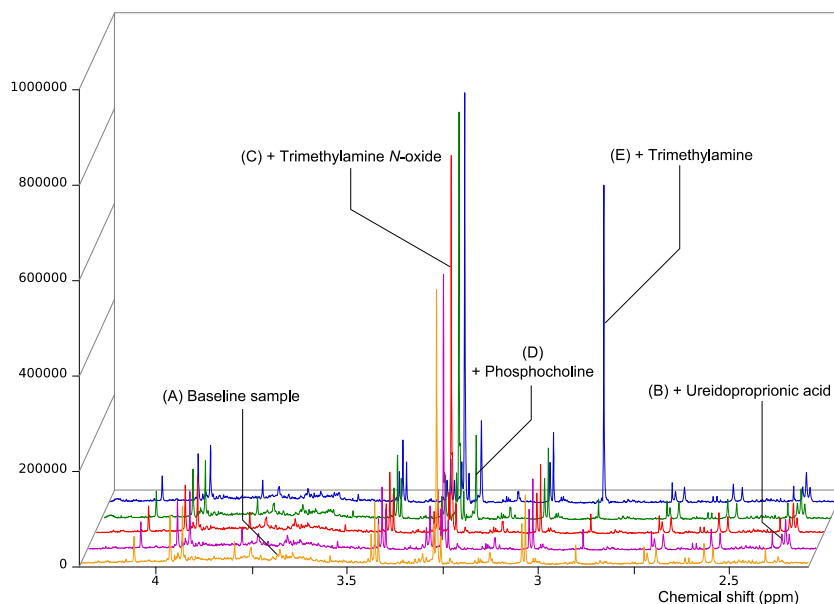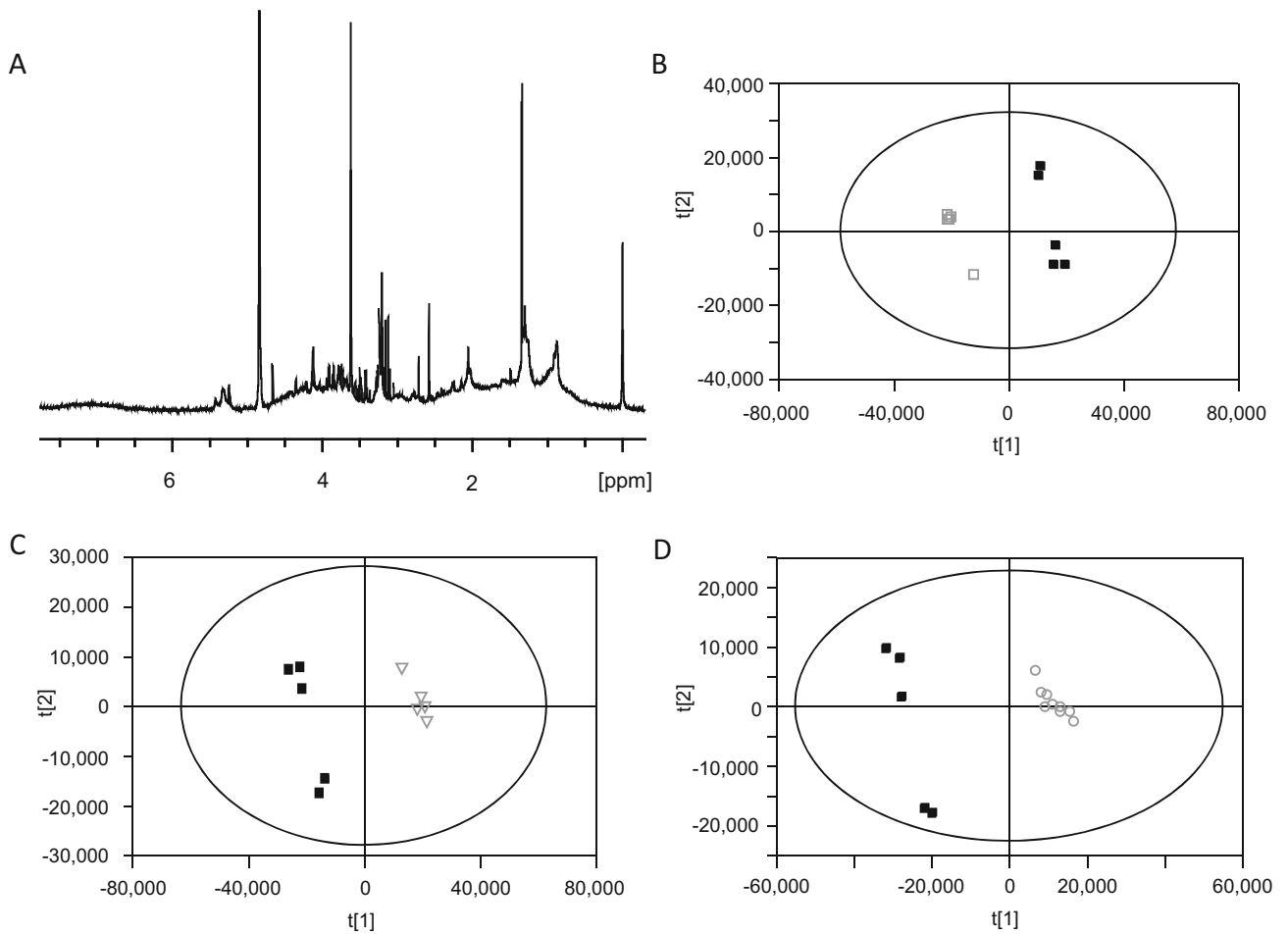
		Day 10	Day 14	Day 28	Day 38
	q²	n.p.	0.44	0.89	0.92
Day 10	↑		Fatty acids; TMAO; phosphocholine	Fatty acids; TMAO	Taurine; TMAO
	↓		Lactate; glucose	Glucose; lactate; choline	Fatty acids; choline; glucose; lactate
	q²	0.54	0.49	0.95	0.62
Day 14	↑		Fatty acids	Fatty acids; choline; TMAO	N-acetyl species; choline; phosphocholine; TMAO; lactate
	↓		Creatine; TMAO; Taurine	Glucose; lactate	Fatty acids
	q²	0.93	0.60	n.p.	0.97
Day 28	↑				Fatty acids; choline
	↓				Glucose; lactate
	q²	0.93	0.92	0.7473	0.97
Day 38	↑				Glucose; N-acetyl species
	↓				

EAE vs EAE   EAE vs CFA   CFA vs CFA

Panel F

		EAE vs Naïve	CFA vs Naïve
	q²	0.72	0.83
Day 10	↑	Glucose; lactate; choline	Fatty acids; choline; glucose; lactate; TMAO
	↓	Phosphocholine; TMAO; fatty acids	
	q²	0.60	0.65
Day 14	↑	Glucose; lactate	Lactate
	↓	Fatty acids; choline; TMAO	Fatty acids; choline; TMAO
	q²	0.52	n.p.
Day 28	↑	Glucose; choline	
	↓	Fatty acids; citrate	
	q²	0.97	0.63
Day 38	↑	Choline; glucose	Choline
	↓	Fatty acids	Fatty acids; N-acetyl species

animals were compared with the naïve cohort it was again possible to separate the animals at all time-points except day 28. For a detailed description of the metabolite changes within the plasma see Fig. 4f.

Discussion

In this study we have demonstrated that through the use of PLS-DA modelling of the ^{1}H-NMR spectra acquired from urine and plasma samples it is possible not only to differentiate Cr-EAE animals from control groups, but also to differentiate between different stages of the Cr-EAE disease time course. For all positive models, the majority of metabolites in the urine or plasma samples eliciting the separations have been identified. Overall, the plasma models were found to provide more robust results than models generated using data from urine samples. Perhaps most surprising was the ability to separate the first phase of disability from the second phase of disability (relapse), which suggests that the underlying disease mechanisms might be different.

We have previously shown, using metabolomic analysis of urine samples, that it is possible to differentiate between inflammatory lesions with distinct histopathology in the basal ganglia induced by injection of adenovirus causing overexpression of either Il-1β or TNF-α (Griffin et al. 2004). On this basis, we hypothesised that it would be possible to follow disease progression in a chronic relapsing remitting model of MS by urine analysis. The results of this study demonstrate that it is possible to generate discriminative models ($q^2 > 0.40$) in some, but not all, cases. It has previously been shown that diet in healthy humans has a greater effect on urine metabolite composition than plasma metabolite composition from the same subject (Walsh et al. 2006). In our study, the diet of the animals is likely to have varied over the disease time course, as they were given access to a mixed high-energy diet to prevent excessive weight loss. Thus, variation in diet may account for the lack of significance in some models. At the same time, urine production varied considerably between animals resulting in variable metabolite dilution. However, it was important to determine whether models could be generated without restricting diet or controlling urine production in order to assess the potential for translation of this approach to the clinic.

Where q^2 values > 0.4 were generated in the urine-based or plasma-based models, separation between the presymptomatic, day 10 time-point and naïve animals was achieved for both Cr-EAE and CFA groups. CFA is key to the induction of EAE as it generates a Th1-type immunological response, and this might be expected to generate some metabolic changes per se ('t Hart et al. 2011). A small drop in weight also accompanied the CFA injection alone. Comparison of Cr-EAE and CFA animals at day 10

did not show significance in the urine analysis, and it is likely that the effects of the CFA injection are still dominant in the metabolite profile at this time-point. The effects of CFA are also clearly identifiable at day 28 demonstrating that the injection of CFA alone causes a shift in the metabolism of the animals.

CFA injections alone have previously been shown to cause lasting effects such as inducing arthritis-like pathology (Fan et al. 2005). However, by day 14 it was possible to generate a predictive model between the Cr-EAE animals and the CFA animals. At this time-point the Cr-EAE animals showed clear clinical signs, usually with complete tail paralysis. Thus, it would be anticipated that any metabolite markers caused by the induction of Cr-EAE would be substantially elevated at this time-point in accord with these behavioural findings. Importantly, at day 28, when the Cr-EAE animals had recovered from the initial phase of disease and showed no overt clinical signs, it was no longer possible to separate the Cr-EAE animals from the CFA and naïve controls. Thus, the changes in the Cr-EAE urine metabolite profile appear to return to normal levels during this remission phase. The analysis of urine did not provide a good model for separating RR from SP MS (Dickens et al. 2014), but the results of the present study suggest that urine analysis by ^{1}H-NMR/PLS-DA might be useful for monitoring relapse in MS where, unless lesions are present in topologically sensitive sites, EDSS scores may be misleading. This is highlighted by the well known clinico-radiological paradox (Barkhof 2002) in which EDSS score does not correlate very well with radiological outcome by MRI.

The plasma models were able to separate all of the Cr-EAE time-points, with significant q^2 values, including separation between time-points when the disease was clinically silent, such as days 10 and 28. It was also possible to separate Cr-EAE from the two control groups, CFA alone and naïve animals, at all of the time-points. As for the urine analysis, it appears that the effects of CFA alone complicated the models in the early phase of the disease. Interestingly, although it was also possible to separate the CFA and naïve groups across most of the time-points (day 10 and 38), these models were driven by fewer metabolites, including glucose, lactate and choline. Whilst glucose and lactate also varied in the Cr-EAE animals, these metabolites changed in the opposite direction, relative to the naïve animals, compared to the CFA animals.

Perhaps the most important result was obtained at day 38 when the Cr-EAE animals entered the first relapse phase, and when the pathology is most relevant to human MS. While this phase is usually less severe than the initial phase of disease in this experimental model, it is hypothesised that disability observed in the subsequent relapse contains a greater element of progressive neuronal damage with less oedema than in the first phase (Ahmed et al. 2001). Furthermore, the use of the acute inflammatory stage of any EAE model has been called in question due to its perceived lack of relevance to the more

chronic condition in MS (Matsumo et al. 2005; Steinman and Zamvil 2005; Ransohoff 2012). However, the Biozzi Cr-EAE has both the acute phases and then a progressive phase of disease with relapse superimposed on top (Amor et al. 2005). This model has been used to assess novel MS therapies such as anti-IL17 and clear differences in neuroinflammation can be observed (Serres et al. 2011; Mardiguian et al. 2013). Using the metabolomics approach it was possible to separate the Cr-EAE animals at this time-point from all other time-points in the disease and also from both of the control groups. Furthermore, Glucose and lactate were decreased at day 38 relative to day 28 in the Cr-EAE animals. This follows a similar pattern observed in humans where glucose and lactate were reduced in the SP-MS patients compared to the RR-MS. Previous studies have demonstrated that if the animals are allowed to survive beyond 35 days they never fully recover to baseline suggesting that the underlying disease is progressing towards a more SP-like phenotype. These metabolite changes may, or may not, arise directly from the CNS disease, and could instead result from a general perturbation of peripheral metabolism owing to either a stress response or alterations in the peripheral immune system(Griffin et al. 2004).

Conclusions

Here we show that a combination of ^{1}H-NMR and PLS-DA modelling can discriminate between different disease states in a clinically relevant model of relapsing MS, and that some of the metabolites that underpin these models are similar to those observed in humans. This finding suggests that the biofluid metabolomics approach together with this animal model could be used to assess future MS therapies aimed at preventing progressive disease. Furthermore, these data support the blood-borne markers for the diagnosis of brain disease allowing a non-invasive and relatively inexpensive method for this type of diagnosis.

References

't Hart BA, Gran B, Weissert R (2011) EAE: imperfect but useful models of multiple sclerosis. Trends Mol Med 17:119–125

Ahmed Z, Gveric D, Pryce G, Baker D, Leonard JP, Cuzner ML (2001) Myelin/Axonal pathology in interleukin-12 induced serial relapses of experimental allergic encephalomyelitis in the lewis rat. Am J Pathol 158:2127–2138

Alvord EC Jr (1984) The challenge: how good a model of MS is EAE today? Prog Clin Biol Res 146:3–5

Amor S, Smith PA, Bert't H, Baker D (2005) Biozzi mice: of mice and human neurological diseases. J Neuroimmunol 165:1–10

Baker D, O'Neill JK, Gschmeissner SE, Wilcox CE, Butter C, Turk JL (1990) Induction of chronic relapsing experimental allergic encephalomyelitis in Biozzi mice. J Neuroimmunol 28:261–270

Bao Q, Feng J, Chen L, Chen F, Liu Z, Jiang B, Liu C (2013) A robust automatic phase correction method for signal dense spectra. J Magn Reson 234:82–89

Barallobre-Barreiro J, Chung Y-L, Mayr M (2013) Proteomics and Metabolomics for Mechanistic Insights and Biomarker Discovery in Cardiovascular Disease. Revista Española de Cardiología (English Edition)

Barkhof F (2002) The clinico-radiological paradox in multiple sclerosis revisited. Curr Opin Neurol 15:239–245

Bielekova B, Martin R (2004) Development of biomarkers in multiple sclerosis. Brain 127:1463–1478

Billiau A, Matthys P (2001) Modes of action of Freund's adjuvants in experimental models of autoimmune diseases. J Leukoc Biol 70:849–860

Brown A, McFarlin D (1981) Relapsing experimental allergic encephalomyelitis in the SJL/J mouse. Laboratory investigation; a journal of technical methods and pathology 45:278–284.

Dickens AM, Larkin JR, Griffin JL, Cavey A, Matthews L, Turner MR, Wilcock GK, Davis BG, Claridge TDW, Palace J, Anthony DC, Sibson NR (2014) A type 2 biomarker separates relapsing-remitting from secondary progressive multiple sclerosis. Neurology 83:1492–1499

Fan WMT (1996) Metabolite profiling by one- and two-dimensional NMR analysis of complex mixtures. Prog Nucl Magn Reson Spectrosc 28:161–219

Fan AY, Lao L, Zhang RX, Zhou AN, Wang LB, Moudgil KD, Lee DYW, Ma ZZ, Zhang WY, Berman BM (2005) Effects of an acetone extract of Boswellia carterii Birdw. (Burseraceae) gum resin on adjuvant-induced arthritis in lewis rats. J Ethnopharmacol 101:104–109

Giovannoni G, Lai M, Kidd D, Thorpe JW, Miller DH, Thompson AJ, Keir G, Feldmann M, Thompson EJ (1997) Daily urinary neopterin excretion as an immunological marker of disease activity in multiple sclerosis. Brain 120(Pt 1):1–13

Griffin JL, Anthony DC, Campbell SJ, Gauldie J, Pitossi F, Styles P, Sibson NR (2004) Study of cytokine induced neuropathology by high resolution proton NMR spectroscopy of rat urine. FEBS Lett 568:49–54

Hassan-Smith G, Wallace GR, Douglas MR, Sinclair AJ (2012) The role of metabolomics in neurological disease. J Neuroimmunol 248:48–52

Heather LC, Wang X, West JA, Griffin JL (2012) A practical guide to metabolomic profiling as a discovery tool for human heart disease. J Mol Cell Cardiol

Jackson SJ, Lee J, Nikodemova M, Fabry Z, Duncan ID (2009) Quantification of myelin and axon pathology during relapsing progressive experimental autoimmune encephalomyelitis in the Biozzi ABH mouse. J Neuropathol Exp Neurol 68:616–625

Kuhle J, Leppert D, Petzold A, Regeniter A, Schindler C, Mehling M, Anthony DC, Kappos L, Lindberg RLP (2011) Neurofilament heavy chain in CSF correlates with relapses and disability in multiple sclerosis. Neurology 76:1206–1213

Lassmann H (1983) Chronic relapsing experimental allergic encephalomyelitis: its value as an experimental model for multiple sclerosis. J Neurol 229:207–220

Lindon JC, Holmes E, Nicholson JK (2001) Pattern recognition methods and applications in biomedical magnetic resonance. Prog Nucl Magn Reson Spectrosc 39:1–40

Mardiguian S, Serres S, Ladds E, Campbell SJ, Wilainam P, McFadyen C, McAteer M, Choudhury RP, Smith P, Saunders F (2013) Anti–IL-17A treatment reduces clinical score and VCAM-1 expression detected by<i>in Vivo</i>magnetic resonance imaging in chronic relapsing EAE ABH mice. Am J Pathol 182:2071–2081

Matsumo Y, Sakuma H, Miyakoshi A, Tsukada Y, Kohyama K, Park IK, Tanuma N (2005) Characterization of relapsing autoimmune encephalomyelitis and its treatment with decoy chemokine receptor genes. J Neuroimmunol 170:49–61

Meyer UA, Zanger UM, Schwab M (2013) Omics and drug response. Annu Rev Pharmacol Toxicol 53:475–502

Mokhtarian F, McFarlin D, Raine C (1984) Adoptive transfer of myelin basic protein-sensitized T cells produces chronic relapsing demyelinating disease in mice

Noseworthy JH, Lucchinetti C, Rodriguez M, Weinshenker BG (2000) Multiple sclerosis. N Engl J Med 343:938–952

Ott M, Demisch L, Engelhardt W, Fischer PA (1993) Interleukin-2, soluble interleukin-2-receptor, neopterin, L-tryptophan and beta 2-microglobulin levels in CSF and serum of patients with relapsing remitting or chronic progressive multiple sclerosis. J Neurol 241: 108–114

Ransohoff RM (2012) Animal models of multiple sclerosis: the good, the bad and the bottom line. Nat Neurosci 15:1074–1077

Salek RM, Xia J, Innes A, Sweatman BC, Adalbert R, Randle S, McGowan E, Emson PC, Griffin JL (2010) A metabolomic study of the CRND8 transgenic mouse model of Alzheimer's disease. Neurochem Int 56:937–947

Serres S, Mardiguian S, Campbell SJ, McAteer MA, Akhtar A, Krapitchev A, Choudhury RP, Anthony DC, Sibson NR (2011) VCAM-1-targeted magnetic resonance imaging reveals subclinical disease in a mouse model of multiple sclerosis. FASEB J

Skov T, van den Berg F, Tomasi G, Bro R (2006) Automated alignment of chromatographic data. J Chemom 20:484–497

Steinman L, Zamvil SS (2005) Virtues and pitfalls of EAE for the development of therapies for multiple sclerosis. Trends Immunol 26:565–571

Walsh M, Brennan L, Malthouse J, Roche H, Gibney M (2006) Effect of acute dietary standardization on the urinary, plasma, and salivary metabolomic profiles of healthy humans. Am J Clin Nutr 84:531

Waterman C, Currie R, Cottrell L, Dow J, Wright J, Waterfield C, Griffin J (2010) An integrated functional genomic study of acute phenobarbital exposure in the rat. BMC Genomics 11:9

Whitaker JN, McKeehan A, Freeman DW (1994) Monoclonal and polyclonal antibody responses to the myelin basic protein epitope present in human urine. J Neuroimmunol 52:53–60

Whitaker JN, Kachelhofer RD, Bradley EL, Burgard S, Layton BA, Reder AT, Morrison W, Zhao GJ, Paty DW (1995) Urinary myelin basic protein-like material as a correlate of the progression of multiple sclerosis. Ann Neurol 38:625–632

Wishart DS et al (2007) HMDB: the Human Metabolome Database. Nucleic Acids Res 35:D521–D526

Wishart DS, Knox C, Guo AC, Eisner R, Young N, Gautam B, Hau DD, Psychogios N, Dong E, Bouatra S (2009) HMDB: a knowledgebase for the human metabolome. Nucleic Acids Res 37:D603

Zamvil S, Nelson P, Trotter J, Mitchell D, Knobler R, Fritz R, Steinman L (1985) T-cell clones specific for myelin basic protein induce chronic relapsing paralysis and demyelination